Transcription Factor Activation Following Exposure of an Intact Lung Preparation to Metallic Particulate Matter

James M. Samet,[1] Robert Silbajoris,[1] Tony Huang,[1] and Ilona Jaspers[2]

[1]Human Studies Division, National Health and Environmental Effects Research Laboratory, Office of Research and Development, U.S. Environmental Protection Agency, Research Triangle Park, North Carolina, USA; [2]Center for Environmental Medicine and Lung Biology, University of North Carolina at Chapel Hill, Chapel Hill, North Carolina, USA

Metallic constituents contained in ambient particulate matter have been associated with adverse effects in a number of epidemiologic, *in vitro*, and *in vivo* studies. Residual oil fly ash (ROFA) is a metallic by-product of the combustion of fossil fuel oil, which has been shown to induce a variety of proinflammatory responses in lung cells. We have examined signaling pathways activated in response to ROFA exposure and recently reported that ROFA treatment activates multiple mitogen-activated protein (MAP) kinases in the rat lung. In the present study we extended our investigations on the mechanism of toxicity of ROFA to include transcription factors whose activities are regulated by MAP kinases as well as possible effectors of transcriptional changes that mediate the effects of ROFA. We applied immunohistochemical methods to detect ROFA-induced activation of nuclear factor-κ B (NFκB), activating transcription factor-2 (ATF-2), c-Jun, and cAMP response element binding protein (CREB) in intact lung tissue and confirmed and characterized their functional activation using DNA binding assays. We performed these studies using a perfused rabbit lung model that is devoid of blood elements in order to distinguish between intrinsic lung cell effects and effects that are secondary to inflammatory cell influx. We report here that exposure to ROFA results in a rapid activation of all of the transcription factors studied by exerting direct effects on lung cells. These findings validate the use of immunohistochemistry to detect transcription factor activation *in vivo* and demonstrate the utility of studying signaling changes in response to environmental exposures. *Key words:* ATF-2, CREB, c-Jun, immunohistochemistry, NFκB, particulate matter, transcription factors. *Environ Health Perspect* 110:985–990 (2002). [Online 15 August 2002]

http://ehpnet1.niehs.nih.gov/docs/2002/110p985-990samet/abstract.html

Numerous studies have reported associations between exposure to ambient levels of particulate matter (PM) and adverse health effects, including elevated rates of cardiopulmonary morbidity and mortality (*1–5*). Although the mechanism(s) of PM toxicity is not known at present, the relatively short time lag between changes in ambient PM levels and the ensuing changes in the incidence of the associated health effects argues in favor of an acute exposure–response relationship. Inflammation is a feature of the toxicity of many environmental exposures and a common acute end point of toxic injury. Therefore, a significant amount of attention has been focused on inflammatory mechanisms of toxicity of ambient PM.

Ambient PM is a complex and varying mixture of organic and inorganic compounds, and no single component in PM has been correlated with the effects of PM exposure. However, epidemiologic findings point to combustion processes as a source of toxic constituents in PM (*6–8*). Fossil fuel combustion generates numerous metallic compounds associated with ambient PM (*9,10*), which have been linked to PM-induced health effects in animals (*11–14*). Residual oil fly ash (ROFA) is an inorganic mixture of metal salts and silicates that is produced during the burning of low-grade oil. Among the metals found in ROFA are vanadium, zinc, iron, and nickel, with oxides and sulfates as the likely dominant speciations (*15*). Because of its origin as an emitted fossil fuel by-product and the fact that it is virtually devoid of organic compounds, ROFA has been used as a model of combustion derived metallic compounds in PM in a number of *in vitro* and *in vivo* toxicologic studies (*11–14,16–19*).

The inflammatory effects of ROFA in pulmonary tissues and cells have been documented in animal studies and include neutrophilic alveolitis, edema, hyperreactivity, and increased susceptibility to microbial infections (*20*). The toxicologic mechanisms responsible for these effects have been proposed to involve alterations in cell signaling that lead to inflammatory mediator expression (*21,22*). Reported changes in signaling at the cellular level induced by ROFA include disruption of tyrosine phosphate metabolism (*21*), activation of phosphorylation-dependent signaling cascades (*23*), and activation of nuclear factor-κ B (NFκB) (*22*).

Transcription factors are DNA-binding proteins that function as modulators of transcriptional expression (*24*). In this manner, transcription factors participate in virtually every facet of cellular function and response to extracellular stimuli. Notably, the expression of proteins that mediate inflammatory reactions, such as chemokines and cytokines, is under the control of specific transcription factors (*25–29*). The activity of transcription factors such as NFκB, activator protein-1 (AP-1), activating transcription factor-2 (ATF-2), and cAMP response element binding protein (CREB) is typically regulated by phosphorylation-dependent events that can include the phosphorylation of the transcription factor itself, which is then followed by its translocation to the nucleus (*30*). Activation of NFκB also involves degradation of its inhibitory subunit IκB (inhibitor-κ B), which results in the subsequent translocation of the p65-p50 NFκB heterodimer to the nucleus (*31*).

The recent advent of new phosphorylation-state–specific antibodies has enabled investigators to detect the activated forms of an increasing number of signaling proteins, such as receptors, kinases, and transcription factors. Our laboratory is interested in the application of these antibodies to the immunodetection of signal transduction activation in lung tissues exposed to pollutants such as ROFA. We recently reported the use of phospho-specific antibodies for the detection of the activation of the mitogen-activated protein (MAP) kinases ERK (extracellular regulated kinases), JNK (c-Jun N-terminal kinase), and P38 in lung tissue from rats exposed to ROFA (*23*). An important limitation of that study and *in vivo* toxicologic work in general has been the inability to distinguish between the direct effect of a toxic insult on the target tissue and secondary effects that are mediated by activated inflammatory cells recruited from the circulation. Specifically addressed in the present study is the issue of the effects of ROFA on the cells of the lung in the absence of inflammatory cells found in the blood. We report here that, using a perfused rabbit lung model that is devoid of blood cells, ROFA induces phosphorylation and functional activation of the transcription factors c-Jun, ATF-2, CREB, and NFκB in lung cells.

Address correspondence to J.M. Samet, U.S. EPA Human Studies Facility, 104 Mason Farm Road, Chapel Hill, NC 27599, USA. Telephone: (919) 966-0665. Fax: (919) 966-6271. E-mail: samet.jim@epa.gov

The authors contributed equally to this manuscript.

Received 15 November 2001; accepted 21 February 2002.

Materials and Methods

Reagents. ROFA was a gift from Gary E. Hatch (U.S. Environmental Protection Agency, Research Triangle Park, NC). ROFA was collected by the Southern Research Institute (Birmingham, AL) on a Teflon-coated fiberglass filter downstream from the cyclone ("scrubber") of an oil-burning power plant in Florida. At the time of collection, the power plant was burning a low-sulfur number 6 residual oil. The temperature of the effluent stream at the time of collection was 204°C (*32*). The physicochemical properties and composition of the ROFA used in these studies have been described elsewhere (*33*). ROFA was approximately 90% soluble in water and had the following ionizable metal content: 188 mg/mL vanadium, 37.5 mg/mL nickel, 35.5 mg/mL iron, 0.803 mg/mL cobalt, 0.464 mg/mL manganese, 0.295 mg/mL copper, 0.180 mg/mL titanium, 0.168 mg/mL chromium. We purchased protease inhibitor cocktail from Calbiochem (San Diego, CA), acrylamide from Boehringer Mannheim (Indianapolis, IN), and SDS-PAGE molecular weight standards and Western blotting supplies from Bio-Rad (Hercules, CA). We quantified protein levels using a Coomasie blue reagent obtained from Bio-Rad. General laboratory reagents were purchased from Sigma Chemical (St. Louis, MO).

The antibodies against phospho-ATF-2, phospho-c-Jun and NFκB (p65) were mouse anti-human monoclonal IgG fractions; anti-phospho-CREB-1 was a goat anti-human polyclonal IgG; and anti-IκBα was a rabbit anti-human polyclonal IgG. All antibodies were purchased from Santa Cruz Biotechnology (Santa Cruz, CA). These antibodies are certified by the supplier to be specific for their intended ligand. The anti-phospho-ATF-2 antibody reacts with Thr-71 phosphorylated ATF-2. The anti-phospho-c-Jun antibody reacts with Ser-63 phosphorylated c-Jun p39 and does not react with either Jun B or Jun D on the analogous serine residues. The anti-phospho-CREB-1 antibody detects phosphorylated Ser-133 of CREB and also the phosphorylated form of CREB-related proteins ATF-1 and cyclic AMP-responsive element modulator (CREM). The anti-NFκB (p65) antibody is not cross-reactive with c-Rel p75 or Rel B p68. IκBα is not cross-reactive with other IκB family members. All antibodies used in this study were affinity purified.

Isolated perfused lung model. The model using a perfused rabbit lung has been previously described (*34*). Briefly, male New Zealand White rabbits (May's Farm, Wilson, NC) weighing 2.5–3.0 kg were heparinized and anesthetized with sodium pentobarbital. After opening the chest wall, the animal was killed by rapid exsanguination from the left ventricle. Stainless-steel cannulae were tied into the left atrium and the main pulmonary artery. The ligature at the pulmonary artery also passed around the aorta to prevent loss of perfusate into the systemic circulation. The pulmonary circulation was washed free of blood before a recirculating flow at 100 mL/min was established using Krebs-Henseleit buffer (82.8 mM sodium chloride, 4.7 mM potassium chloride, 2.4 mM monobasic potassium phosphate, 25 mM sodium bicarbonate, 1.2 mM magnesium sulfate, 2.7 mM calcium chloride, and 11.1 mM dextrose) containing 3% bovine serum albumin (BSA) at a temperature of 37–38°C and pH 7.3–7.4. The perfusion circuit consisted of a reservoir, a roller pump (Sarns, Inc., Ann Arbor, MI), and a bubble trap and a heat exchanger, connected with Tygon tubing (Model FT100; Grass Instrument Company, Quincy, MA). The reservoir was placed at the lowest portion of the lung to maintain a left atrial pressure of zero. The volume of the system was approximately 250 mL. The lung was ventilated with 21% O_2 + 5% CO_2 through a tracheostomy using an animal respirator (Harvard Apparatus Company, Inc., Holliston, MA) delivering 30 breaths/min at 2 cm H_2O positive end-expiratory pressure. We adjusted the tidal volume to achieve a peak tracheal pressure (P_{AW}) of 7–10 mm Hg (~20 mL). The mean pulmonary artery pressure (P_{PA}) and P_{AW} were recorded on a four-channel recorder (Model 2450S; Gould Inc., Cleveland, OH) continuously using pressure transducers (P231D; Gould Statham Instruments, Inc., Hato Ray, Puerto Rico). After establishment of recirculating flow, the lung was allowed 10 min for stabilization. We excluded lungs with visible leaks and/or high pulmonary artery pressure (> 20 mm Hg) during this period. Two animals were used per treatment reported in this study.

In vivo *ROFA exposure.* We administered 2 mg of ROFA suspended in 2 mL sterile 0.9% NaCl by intratracheal instillation. The tracheostomy tube was disconnected briefly from the ventilator circuit to allow the lung to deflate completely. The solution was then instilled into the distal trachea, and the lung was reinflated and ventilation reestablished to allow the suspended ROFA to be distributed to the distal lung regions. Instillation of ROFA was followed by 40 min of perfusion. Previous studies had established that the viability of the system was stable for at least 2 hr. We chose the 40-min time point to accommodate the rapid nature of signaling events while minimizing the risk of secondary effects. Control lungs were treated with 2 mL of sterile 0.9% NaCl using the same delivery method as that for the ROFA-treated lungs.

Separation of cytoplasmic and nuclear protein fractions. Frozen rabbit lung tissues were homogenized on ice in CEB buffer (10 mM Tris, pH 7.9, 60 mM potassium chloride, 1 mM EDTA, and 1mM dithiothreitol) containing an antiprotease cocktail (1 mM 4-(2-aminoethyl)benzene sulfonyl fluoride, 0.8 μM aprotinin, 20 μM leupeptin, 50 μM bestatin, 10 μM pepstatin A, 15 μM L-*trans*-epoxy succinyl-leucyl-amido (4-guanidino) butane, 1 mM phenylmethyl sulfonyl fluoride, 1 mM sodium fluoride, and 1 mM vanadyl sulfate. After a 10-min incubation on ice, nonidet P-40 (0.2%) was added and the samples were mixed well and then centrifuged at 16,000 × *g* for 1 min at 4°C. The nuclear pellet was washed once with cold CEB buffer and recentrifuged at 16,000 × *g* for 5 min at 4°C. The pellet was resuspended in NEB buffer (20 mM Tris, pH 8.0; 400 mM NaCl; 1.5 mM $MgCl_2$; 1.5 mM EDTA; 25% glycerol; and 1 mM DTT) containing protease inhibitors, 1 mM sodium fluoride and 1mM vanadyl sulfate, and incubated on ice for 10 min. Samples were centrifuged at 10,000 × *g* for 10 min, and the supernatants containing extracted nuclear proteins were aliquoted and stored at –80°C.

Western blotting. We determined levels of IκBα and phosphorylated ATF-2, c-Jun, and CREB-1 in control and ROFA-treated rabbit lungs by SDS-PAGE. For IκBα analyses, frozen lung tissues were homogenized on ice in RIPA lysis buffer [0.1% SDS, 0.5% deoxycholate, 1% Nonidet P-40 in phosphate buffered saline (PBS), pH 7.4], containing an antiprotease cocktail (*35*) and 1 mM vanadyl sulfate. Homogenates were centrifuged at 10,000 × *g* for 10 min, and the supernatants were aliquoted and stored at –80°C. Nuclear protein fractions extracted from frozen lung tissues were used for phosphorylated ATF-2, c-Jun, and CREB-1 analyses.

Samples were mixed with an equal volume of SDS-PAGE loading buffer (0.125 M Tris, pH 6.8, 4% SDS, 20% glycerol, 10% β-mercaptoethanol, and 0.05% bromophenol blue), boiled for 5 min, and separated on 11% SDS-PAGE gels in Tris-glycine-SDS buffer (*36*). We ran prestained molecular weight markers on adjacent lanes. We used 50 μg of whole-lung homogenates for the analysis of IκBα. We used 20 μg of nuclear protein extracts for the analyses of phosphorylated ATF-2, c-Jun, and CREB-1. Electrophoresed proteins were electro-blotted onto nitrocellulose (*37*). Blots were blocked with 3% casein in 50 mM PBS, pH 7.4 for 1 hr, washed briefly with PBS-0.05% Tween-20, and incubated overnight at 4°C with primary antibody in 5% BSA in PBS-Tween. Blots were washed, then incubated with horseradish peroxidase (HRP)-conjugated secondary antibody (Santa Cruz Biotechnology) in 3% casein in PBS-Tween for 1 hr at room temperature. Antibodies were used at concentrations between 0.5 and 1.0 μg/mL. We detected protein bands using chemiluminescence reagents and film as per manufacturer's instructions (Amersham Life

Science, Arlington Heights, IL). Images were digitized with a Kodak DC120 digital camera using the Kodak Digital Science Electrophoresis Documentation and Analysis System 120 (Eastman Kodak, Rochester, NY).

Electrophoretic mobility shift assay. We used nuclear protein samples extracted from control and ROFA-exposed rabbit lungs in electrophoretic mobility shift assay (EMSA). DNA binding activities to the major histocompatibility complex (MHC) class II NFκB response element were performed as described previously (*38*). AP-1 and ATF-2/CREB-1 DNA binding activities were performed using commercially available EMSA kits for the respective transcription factors (Nushift kits; Geneka Biotechnology, Montreal, Canada) according to the suppliers instructions. All DNA–protein samples were separated by electrophoresis through 4.5% nondenaturing polyacrylamide gels containing 0.5X Tris/glycine/EDTA at 4°C. Gels were dried, and radiolabeled DNA–protein complexes were autoradiographed using a PhosphorImager (Molecular Dynamics, Sunnyvale, CA). The nucleotide sequences used were ATF-2/CREB-1 (5′-GATTCA ATGACATCACGGCTGTG-3′), AP-1 (5′-CGCTTGATGAGTCAGCCGGAA-3′), and NFκB (5′-GGCTGGGGATTCCC-CATCT-3′).

Immunohistochemistry. After exposure to ROFA or saline, rabbit lungs were inflation fixed with 4% paraformaldehyde at 20 cm fixative pressure overnight at 4°C. Lungs were transferred to PBS and processed for paraffin embedding. We cut 4-μm sections using a Leica RM 2155 microtome (Leica, Deerfield, IL) onto Fisher Superfrost Plus slides (Fisher Scientific, Pittsburgh, PA). Sections were deparaffinized by heating at 60°C for 45 min and washing twice with xylene, rehydrated in a graded series of ethanol, and washed in Tris-buffered saline, pH 8.0 (TBS). We performed antigen retrieval (unmasking) on lung sections before incubation with antibodies. After rehydration, sections were placed in 0.1 M citric acid, pH 6.0, heated in a microwave at high power for 50 sec, followed by low power for 15 min. After cooling, the sections were rinsed with H_20 and washed in TBS.

Prediluted immunohistochemical reagents [endogenous peroxidase block, normal serum block, HRP-streptavidin and diaminobenzidine (DAB)] were from an ImmunoCruz Staining System kit (Santa Cruz Biotechnology). Immunostaining was done as follows: a 10-min endogenous peroxidase block was followed by three 5-min washes in TBS-0.1% Triton X-100 (TBST) and a 90-min block with normal goat or donkey serum. Lung sections were then incubated overnight at 4°C with primary antibodies diluted with TBST-3% BSA [anti-phospho-ATF-2 (160 μg/mL), anti-phospho-c-Jun (160 μg/mL), anti-NFκB (p65; 80 μg/mL), anti-phospho-CREB-1 (20 μg/mL)], washed three times for 5 min with TBST, incubated with the appropriate biotin-conjugated secondary antibody [goat anti-mouse IgG, human, mouse and rat serum-adsorbed (Sigma Chemical) or donkey anti-goat IgG, human, mouse, rat, and rabbit serum-adsorbed (Jackson ImmunoResearch Laboratories, West Grove, PA)] washed three times for 5 min with TBST, incubated 30 min with HRP-streptavidin, washed two times 5 min with TBST, washed once for 5 min with water, and incubated 10 min with DAB.

Normal goat and mouse IgG sera were diluted to the same protein concentrations as the primary antibodies and routinely used as negative controls.

Sections were mounted with Crystal/Mount (Biomeda, Foster City, CA); photographs were taken with a Nikon Coolpix 990 digital camera attached to a Nikon E600 light microscope (Nikon, Tokyo, Japan) under differential interference contrast illumination. We edited the resulting images for manuscript preparation using Adobe Photoshop (Adobe Systems, San Jose, CA).

Results

To determine the direct effect of ROFA on the activation of signaling intermediates in the lung, isolated, perfused rabbit lungs were instilled with ROFA or vehicle and subjected to immunohistochemical, Western blotting, and DNA binding analyses. Lung tissue immunostaining for NFκB (p65), phospho-ATF-2, phospho-c-Jun, and phospho-CREB was increased in rabbits exposed to ROFA compared to controls (Figure 1). Bronchial epithelial cells stained positively with all the transcription factor antibodies. Nuclear and perinuclear staining was apparent for NFκB (p65), consistent with the activation of the NFκB pathway. The extent of staining of the alveolar epithelium varied. NFκB (p65) showed almost no alveolar staining, and phospho-ATF-2 and phospho-c-Jun staining was patchy. The immunostaining of phospho-CREB was diffuse in the alveolar region. Alveolar macrophages were positive for

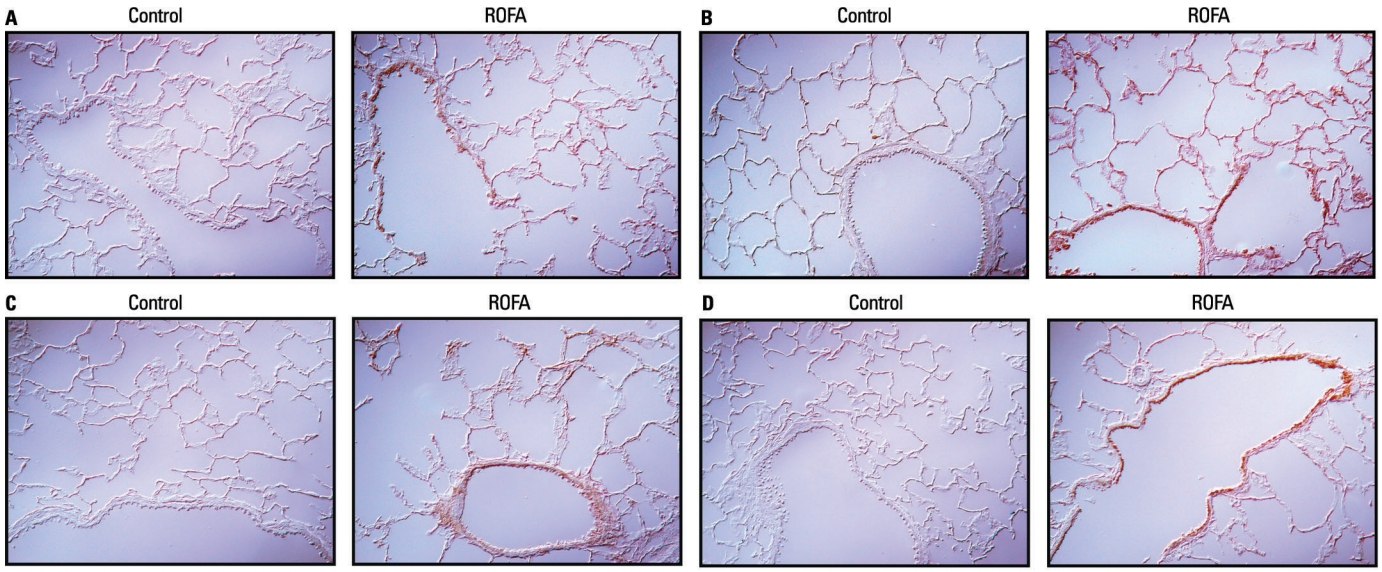

Figure 1. Immunohistochemical detection of transcription factor activation in perfused rabbit lung tissue following exposure to ROFA. See "Materials and Methods" for details. Fixed and embedded lung sections were incubated with specific (*A*) anti-phospho-ATF-2, (*B*) anti-phospho-CREB, (*C*) anti-phospho-c-Jun, or (*D*) anti-p65 antibodies, followed by biotin-conjugated secondary antibodies. Detection of immune complexes was accomplished using HRP-conjugated streptavidin and diaminobenzidine. Sections show both airway and alveolar tissue.

phospho-ATF-2, phospho-c-Jun, and phospho-CREB. There was no staining for any of the transcription factors in blood vessels or bronchial smooth muscle. The change in the p65 signal appears to represent an actual increase in immunostaining and not a change in the ratio of cytosolic to nuclear localization of this NFκB subcomponent (Figure 1). A summary of the staining pattern in the lung for each transcription factor is shown in Table 1.

To corroborate and complement the immunohistochemical findings, we used Western blotting to detect evidence of ROFA-induced activation of transcription factors in perfused rabbit lung tissue. Total or nuclear protein extracts prepared from homogenates of rabbit lung exposed to vehicle or ROFA were fractionated by SDS PAGE and immunoblotted using specific antibodies. These analyses verified that exposure to ROFA induced marked activation of ATF-2, c-Jun, and CREB, as evidenced by increases in nuclear levels of the phosphorylated forms of these transcription factors (Figure 2). Activation of NFκB in the rabbit lung tissue was shown by a ROFA-induced degradation of the inhibitory subunit IκBα, an event known to precede the nuclear translocation of the p65–p50 heterodimer (Figure 2).

We used EMSAs to determine whether exposure to ROFA induces a functional activation of transcription factors in the perfused rabbit lung model. Total lung homogenates from rabbits exposed to ROFA or vehicle alone were prepared and nuclear proteins were then extracted and assayed for specific DNA-binding activity to oligonucleotide sequences found in various response elements. As shown in Figure 3, exposure to ROFA induced a pronounced increase in the DNA-binding activity of NFκB to the MHC class II NFκB response element. Similar increases in DNA-protein binding were observed using an AP-1 response element, targeted by phospho-c-Jun-containing homo and heterodimers, and an oligonucleotide recognized by both ATF-2 and CREB-1 (Figure 3).

We further characterized the ROFA-induced transcription factor DNA binding detected by EMSA using an excess of specific competitive oligonucleotides and specific antibodies. The intensity of the EMSA shift of the NFκB oligonucleotide probe was strongly reduced with the use of an excess of unlabeled ("cold") wild-type probe. However, competition with an unlabeled oligonucleotide that differs from the probe sequence by a single nucleotide (mutant NFκB) produced only a partial reduction in the intensity of the EMSA signal (Figure 4A). Further identification of the NFκB subunits involved in the DNA binding induced by ROFA exposure was performed using specific antibodies against the NFκB family members p65, p50, and c-Rel. An antibody against p65 was effective in enhancing the retardation ("supershifting") of a major band induced by ROFA treatment. In contrast, antibodies against p50 and c-Rel did not alter the EMSA binding pattern induced by ROFA (Figure 4A). Supershifting of a major DNA-binding complex band was seen with an anti-phospho-c-Jun antibody, confirming the presence of activated c-Jun in the AP-1 DNA-binding complex (Figure 4B). As shown in Figure 4C, the specificity of the ATF-2/CREB binding induced by ROFA exposure was also shown by competition with wild-type and mutant oligonucleotides. Antibodies against phospho-ATF-2 caused a detectable supershift of the complex, while an anti-phospho-CREB antibody produced no change in the EMSA pattern (Figure 4C).

Discussion

A number of *in vitro* and *in vivo* studies have demonstrated the inflammatory effect of exposure to ambient particulate matter components in the lung (*11,14,39–41*). An important mechanistic issue that remained to be addressed was distinguishing between the direct effects of the exposure on lung cells and those that are secondary to the infiltration and activation of inflammatory cells derived from the blood. Although the possibility remains of cell-to-cell trans-stimulation within the lung by resident macrophages and neutrophils, the data from the present study using a perfused lung model establish that exposure to the metallic PM mixture ROFA induces direct activation of intracellular signaling in lung cells that does not require participation by extrapulmonary cells.

The observation that the immunostaining for transcription factor activation induced by ROFA occurs predominantly in the airway epithelium is likely a reflection of the pattern and dosimetry of the deposition of instilled ROFA in the lung. However, it may also be underlain by a differential susceptibility of the airway epithelial cells when compared to the alveolar cells to this type of stimulation. The accumulation of phosphorylated proteins in rabbit lung tissue shown by increased immunohistochemical staining can be thought of as a broad marker of intracellular signal transduction activation. ROFA has previously been shown to cause increases in protein phosphotyrosines in a human airway epithelial cell line (*21*) and in the rat lung (*23*). In human airway epithelial cells, the mechanism responsible for this effect is a dysregulation of phosphotyrosine metabolism resulting from a vanadium-induced inhibition of tyrosine phosphatases (*21*). Thus, although the mechanistic link between transcription factor phosphorylation and the activation of upstream kinases was not established here, it is likely that the phosphorylation-dependent activation of the transcription factors reported in this study reflects a dysregulation of phosphotyrosine metabolism caused by inhibition of tyrosine phosphatases. Furthermore, it is reasonable to speculate that vanadium is the constituent in ROFA that induces the activation of these transcription factors in the perfused rabbit lung model, as it was in the *in vitro* study.

NFκB activation mediates critical cellular responses that control gene expression and programmed cell death (*28*). In human airway epithelial cells, NFκB has been associated with the expression of interleukin-6 (IL-6) in response to ROFA exposure (*22*). Levels of IL-6 and other mediators have also been seen to increase in the bronchoalveolar lavage fluid of animals instilled with ROFA (*11,42*). Thus, the increase in NFκB activation observed in this study may be an event that

Table 1. Summary of immunohistochemical findings in tissue sections of rabbit lung exposed to ROFA.

Antibody	Bronchial epithelium	Alveolar epithelium	Alveolar macrophages	Blood vessels	Bronchial smooth muscle
NFκB (p65)	++	–	–	–	–
Phospho-ATF-2	+	+	+	–	–
Phospho-c-Jun	+	+	+	–	–
Phospho-CREB	++	+	++	–	–

Arbitrary estimations of the relative intensity of transcription factor immunostaining associated with lung histologic features are denoted as undetected (–), low (+), or high (++). Comparisons are only valid for the same antibody and therefore should only be made within rows and not across different transcription factors.

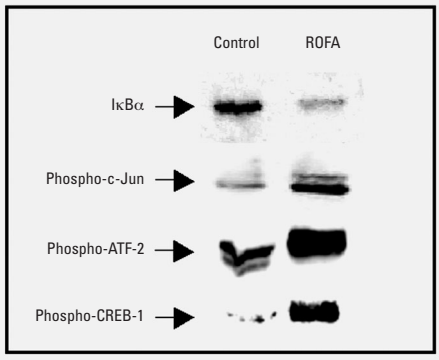

Figure 2. Transcription factor activation in homogenized perfused rabbit lung tissue after exposure to ROFA. See "Materials and Methods" for details. Lung tissue was homogenized and subjected to SDS-PAGE followed by Western blotting analyses using anti-IκBα (40 kD), anti-phospho-c-Jun (39 kD), anti-phospho-ATF-2 (68–72 kD), or anti-phospho-CREB (43 kD) antibodies.

leads to cytokine expression in the perfused rabbit lung model as well. Vanadium exposure has been shown to effectively reproduce the effects of ROFA on NFκB *in vitro* (*38,43*), suggesting that vanadium is a primary active component in ROFA that directly mediates NFκB activation in the perfused rabbit lung model. Although certain vanadium compounds are proposed to induce activation of NFκB through an alternate pathway that does not involve degradation of the inhibitory subunit IκBα (*44,45*), the fact that Western blotting showed reduced levels of IκBα in homogenates from ROFA-treated lungs is consistent with activation of the classical pathway for NFκB activation (*43*). However, the supershift data suggest that the presence of a p65 homodimer in the ROFA-induced DNA-binding complex in the rabbit lung. Additional work will be needed to establish the significance of this finding.

c-Jun is a specific substrate of JNK, whereas ATF-2 can be phosphorylated by either JNK or p38 (*46*). Thus, the activation of these transcription factors is likely a consequence of the activation of these MAP kinases in the perfused rabbit lung exposed to ROFA. The induction of c-Jun and ATF-2 phosphorylation in the ROFA-treated perfused rabbit lung reported here is, therefore, consistent with our previous report of the activation of the MAP kinases JNK and p38 in lung tissue of rats intratracheally instilled with ROFA (*23*). In contrast, CREB is a transcription factor linked to cAMP generation and protein kinase A activation (*47*), which has not been previously reported to be activated in response to ROFA or metallic exposure.

In general, the DNA-binding activity measured in this study can be viewed as corroborative of the immunostaining and Western blot findings, reducing the likelihood that they are the result of artifacts of the immunohistochemical processing. Functional activation of the NFκB pathway in the perfused rabbit lung tissue by ROFA is clearly demonstrated by the EMSA results showing enhanced binding to an NFκB-specific oligonucleotide sequence. In addition, the supershift findings showed active p65 in the DNA binding complex. The AP-1 EMSA data similarly support an increase in a functionally active phospho-c-Jun in the ROFA-exposed rabbit lung. In the case of ATF-2 and CREB-1, both recognize the same nucleotide sequence used in the present study, and the ROFA-induced increase in DNA binding demonstrated by EMSA could, therefore, represent binding by either or both transcription factors. The supershift data demonstrated the involvement of ATF-2, but not CREB, in the DNA-binding complex induced in the ROFA-exposed rabbit lung. This apparent discrepancy between the immunostaining and EMSA findings may reflect a lack of functional activation of the phosphorylated CREB induced by ROFA, in the face of immunohistochemical and Western blotting data showing ROFA-induced phosphorylation of CREB. However, we cannot rule out the possibility that the failure to obtain a CREB supershift is due to a limitation of the antibody used in this experiment. In any case, these data show the value of using multiple complementary methods to evaluate the state of activation of transcription factors.

c-Jun is a component of the AP-1 heterodimer that binds to the ternary complex response element/AP-1 DNA response element (*48*). AP-1 activation has been linked to IL-6 and IL-8 expression in a number of cell types (*49–52*), and may, therefore, also contribute to ROFA-induced inflammatory reactions in the lung. Likewise, ATF-2 activation is involved in the expression of tumor necrosis factor α (*53*) and adhesion molecules (*54*). Like c-Jun, ATF-2 is capable of binding to AP-1; however, it can bind to the CRE response element as well (*46,55*). CREB-mediated transcription is associated with diverse cellular responses, including intermediary metabolism, neuronal signaling, cell proliferation, and apoptosis (*56–58*). Additional studies will be needed to identify associations between individual responses and the activation of specific transcription factors such as CREB, ATF-2, and c-Jun by ROFA exposure *in vitro* and *in vivo*.

In summary, we have shown here that ROFA induces the phosphorylation and functional activation of multiple transcription factors that are associated with proinflammatory responses by lung cells in the absence of blood elements. These findings imply that the response to combustion-derived metallic mixtures found in ambient PM involves a direct alteration of transcriptional regulators in target cells in the lung and thus suggest a potential mechanism for the health effects of PM inhalation.

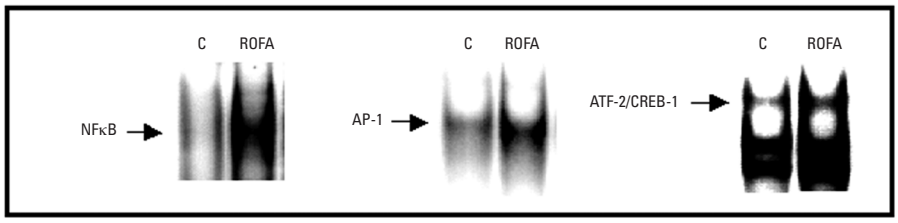

Figure 3. DNA binding activity of nuclear proteins in rabbit lung tissue after exposure to ROFA. C, control. See "Materials and Methods" for details. Lung tissue was homogenized and nuclear proteins were extracted and subjected to analysis by EMSA using specific radiolabeled oligonucleotide probes corresponding to NFκB, AP-1, or AF-2/CREB response elements.

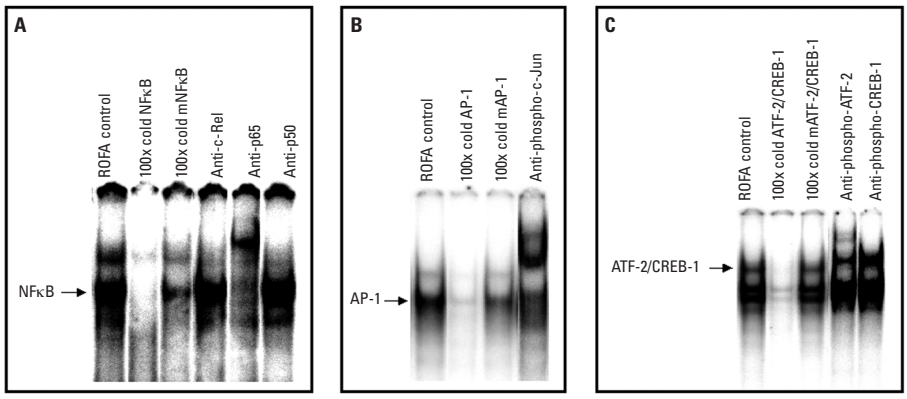

Figure 4. Characterization of the DNA binding activity induced by ROFA exposure. (*A*) NFκB. (*B*) AP-1. (*C*) ATF-2/CREB-1. EMSAs were performed on nuclear extracts from ROFA-exposed rabbit lung tissue as described in "Materials and Methods." The DNA binding reactions were performed in the presence of either vehicle (ROFA control), 100-fold excess unlabeled wild-type probe, 100-fold excess unlabeled mutant probe, or the specified antibodies.

References and Notes

1. Samet JM, Dominici F, Curriero FC, Coursac I, Zeger SL. Fine particulate air pollution and mortality in 20 U.S. cities, 1987-1994. N Engl J Med 343:1742–1749 (2000).
2. Schwartz J. What are people dying of on high air pollution days? Environ Res 64:26–35 (1994).
3. Schwartz J. Particulate air pollution and daily mortality: a synthesis. Public Health Rev 19:39–60 (1991).
4. Dockery DW, Speizer FE, Stram DO, Ware JH, Spengler JD, Ferris BG Jr. Effects of inhalable particles on respiratory health of children. Am Rev Respir Dis 139:587–594 (1989).
5. Dockery DW, Brunekreef B. Longitudinal studies of air pollution effects on lung function. Am J Respir Crit Care Med 154:S250–S256 (1996).
6. Laden F, Neas LM, Dockery DW, Schwartz J. Association of fine particulate matter from different sources with daily mortality in six U.S. cities. Environ Health Perspect 108:941–947 (2000).

7. Schwartz J, Dockery D, Neas LM. Is daily mortality associated specifically with fine particles? J Air Waste Manag Assoc 46:927–939 (1996).
8. Yu O, Sheppard L, Lumley T, Koenig JQ, Shapiro GG. Effects of ambient air pollution on symptoms of asthma in Seattle-area children enrolled in the CAMP study. Environ Health Perspect 108:1209–1214 (2000).
9. Frampton MW, Ghio AJ, Samet JM, Carson JL, Carter JD, Devlin RB. Effects of aqueous extracts of PM_{10} filters from the Utah valley on human airway epithelial cells. Am J Physiol 277:L960–L967 (1999).
10. Costa DL, Dreher KL. Bioavailable transition metals in particulate matter mediate cardiopulmonary injury in healthy and compromised animal models. Environ Health Perspect 105(suppl 5):1053–1060 (1997).
11. Dreher K, Jaskot R, Kodavanti U, Lehmann J, Winsett D, Costa D. Soluble transition metals mediate the acute pulmonary injury and airway hyperreactivity induced by residual oil fly ash articles. Chest 109:33S–34S (1996).
12. Dye JA, Adler KB, Richards JH, Dreher KL. Role of soluble metals in oil fly ash-induced airway epithelial injury and cytokine gene expression. Am J Physiol 277:L498–L510 (1999).
13. Gavett SH, Madison SL, Stevens MA, Costa DL. Residual oil fly ash amplifies allergic cytokines, airway responsiveness, and inflammation in mice. Am J Respir Crit Care Med 160:1897–1904 (1999).
14. Kodavanti UP, Jaskot RH, Bonner J, Badgett A, Dreher KL. Eosinophilic lung inflammation in particulate-induced lung injury: technical consideration in isolating RNA for gene expression studies. Exp Lung Res 22:541–554 (1996).
15. Henry WM, Knapp KT. Compound forms of fossil fuel fly ash emissions. Environ Sci Technol 14:450–456 (1980).
16. Watkinson WP, Campen MJ, Costa DL. Cardiac arrhythmia induction after exposure to residual oil fly ash particles in a rodent model of pulmonary hypertension. Toxicol Sci 41:209–216 (1998).
17. Longphre M, Li D, Li J, Matovinovic E, Gallup M, Samet JM, Basbaum CB. Lung mucin production is stimulated by the air pollutant residual oil fly ash. Toxicol Appl Pharmacol 162:86–92 (2000).
18. Samet JM, Ghio AJ, Costa DL, Madden MC. Increased expression of cyclooxygenase 2 mediates oil fly ash-induced lung injury. Exp Lung Res 26:57–69 (2000).
19. Ghio AJ, Carter JD, Richards JH, Crissman KM, Bobb HH, Yang F. Diminished injury in hypotransferrinemic mice after exposure to a metal-rich particle. Am J Physiol Lung Cell Mol Physiol 278:L1051–L1061 (2000).
20. Pritchard RJ, Ghio AJ, Lehman JR, Winsett DW, Tepper JS, Park P, Gilmour MI, Dreher KL, Costa D. Oxidant generation and lung injury after particulate air pollutant exposure increase with the concentrations of associated metals. Inhal Toxicol 8:457–477 (1996).
21. Samet JM, Stonehuerner J, Reed W, Devlin RB, Dailey LA, Kennedy TP, Bromberg PA, Ghio AJ. Disruption of protein tyrosine phosphate homeostasis in bronchial epithelial cells exposed to oil fly ash. Am J Physiol Lung Cell Mol Physiol 272:L426–L432 (1997).
22. Quay JL, Reed W, Samet J, Devlin RB. Air pollution particles induce IL-6 gene expression in human airway epithelial cells via NF-kappaB activation. Am J Respir Cell Mol Biol 19:98–106 (1998).
23. Silbajoris R, Ghio AJ, Samet JM, Jaskot R, Dreher KL, Brighton LE. In vivo and in vitro correlation of pulmonary MAP kinase activation following metallic exposure. Inhal Toxicol 12:453–468 (2000).
24. Krauss G. Biochemistry of Signal Transduction and Regulation. Weinheimm, Germany:Wiley-VCH, 1999.
25. Roebuck KA. Regulation of interleukin-8 gene expression. J Interferon Cytokine Res 19:429–438 (1999).
26. Driscoll KE, Carter JM, Hassenbein DG, Howard B. Cytokines and particle-induced inflammatory cell recruitment. Environ Health Perspect 105(suppl 5):1159–1164 (1997).
27. Barnes PJ. Air pollution and asthma: molecular mechanisms. Mol Med Today 1:149–155 (1995).
28. Baldwin AS Jr. Series introduction: the transcription factor NF-kappaB and human disease. J Clin Invest 107:3–6 (2001).
29. Akira S, Isshiki H, Nakajima T, Kinoshita S, Nishio Y, Natsuka S, Kishimoto T. Regulation of expression of the interleukin 6 gene: structure and function of the transcription factor NF-IL6. Ciba Found Symp 167:47–62 (1992).
30. Whitmarsh AJ, Davis RJ. Regulation of transcription factor function by phosphorylation. Cell Mol Life Sci 57:1172–1183 (2000).
31. Israel A. A role for phosphorylation and degradation in the control of NF-kappa B activity. Trends Genet 11:203–205 (1995).
32. Hatch GE, Boykin E, Graham JA, Lewtas J, Pott F, Loud K, Mumford JL. Inhalable particles and pulmonary host defense: in vivo and in vitro effects of ambient air and combustion particles. Environ Res 36:67–80 (1985).
33. Pritchard RJ, Ghio AJ, Lehman JR, Winsett DW, Tepper JS, Park P, Gilmour MI, Dreher KL, Costa D. Oxidant generation and lung injury after particulate air pollutant exposure increase with the concentrations of associated metals. Inhal Toxicol 8:457–477 (1996).
34. Huang YC, Fisher PW, Nozik-Grayck E, Piantadosi CA. Hypoxia compared with normoxia alters the effects of nitric oxide in ischemia-reperfusion lung injury. Am J Physiol 273:L504–L512 (1997).
35. Samet JM, Ghio AJ, Madden MC. Increased Expression of Cyclooxygenase 2 Mediates Oil Fly Ash-Induced Lung Injury. Exp Lung Res 26:57–69 (2000).
36. Laemmli UK. Cleavage of structural proteins during the assembly of the head of bacteriophage T4. Nature 227:680–685 (1970).
37. Towbin H, Staehelin T, Gordon J. Electrophoretic transfer of proteins from polyacrylamide gels to nitrocellulose sheets: procedure and some applications. Proc Natl Acad Sci USA 76:4350–4354 (1979).
38. Jaspers I, Samet JM, Reed W. Arsenite exposure of cultured airway epithelial cells activates kappaB-dependent interleukin-8 gene expression in the absence of nuclear factor-kappaB nuclear translocation. J Biol Chem 274:31025–31033 (1999).
39. Adamson IY, Prieditis H, Hedgecock C, Vincent R. Zinc is the toxic factor in the lung response to an atmospheric particulate sample. Toxicol Appl Pharmacol 166:111–119 (2000).
40. Dye JA, Lehmann JR, McGee JK, Winsett DW, Ledbetter AD, Everitt JI, Ghio AJ, Costa DL. Acute pulmonary toxicity of particulate matter filter extracts in rats: coherence with epidemiologic studies in Utah Valley residents. Environ Health Perspect 109(suppl 3):395–403 (2001).
41. Frampton MW, Ghio AJ, Samet JM, Carson JL, Carter JD, Devlin RB. Unpublished data.
42. Kodavanti UP, Jaskot RH, Costa DL, Dreher KL. Pulmonary proinflammatory gene induction following acute exposure to residual oil fly ash—roles of particle-associated metals. Inhal Toxicol 9:679–701 (1997).
43. Jaspers I, Samet JM, Erzurum S, Reed W. Vanadium-induced κB-dependent transcription depends upon peroxide-induced activation of the p38 mitogen-activated protein kinase. Am J Respir Cell Mol Biol 23:95–102 (2000).
44. Imbert V, Peyron JF, Farahi Far D, Mari B, Auberger P, Rossi B. Induction of tyrosine phosphorylation and T-cell activation by vanadate peroxide, an inhibitor of protein tyrosine phosphatases. Biochem J 297:163–173 (1994).
45. Singh S, Darnay BG, Aggarwal BB. Site-specific tyrosine phosphorylation of IκBα negatively regulates its inducible phosphorylation and degradation. J Biol Chem 271:31049–31054 (1996).
46. Wilhelm D, van Dam H, Herr I, Baumann B, Herrlich P, Angel P. Both ATF-2 and c-Jun are phosphorylated by stress-activated protein kinases in response to UV irradiation. Immunobiology 193:143–148 (1995).
47. Montminy M. Transcriptional regulation by cyclic AMP. Annu Rev Biochem 66:807–822 (1997).
48. Whitmarsh AJ, Davis RJ. Transcription factor AP-1 regulation by mitogen-activated protein kinase signal transduction pathways. J Mol Med 74:589–607 (1996).
49. Munoz C, Pascual-Salcedo D, Castellanos MC, Alfranca A, Aragones J, Vara A, Redondo MJ, de Landazuri MO. Pyrrolidine dithiocarbamate inhibits the production of interleukin-6, interleukin-8, and granulocyte-macrophage colony-stimulating factor by human endothelial cells in response to inflammatory mediators: modulation of NF-kappa B and AP-1 transcription factors activity. Blood 88:3482–3490 (1996).
50. Jaspers I, Flescher E, Chen LC. Ozone-induced IL-8 expression and transcription factor binding in respiratory epithelial cells. Am J Physiol 272:L504–L511 (1997).
51. Tanaka C, Kamata H, Takeshita H, Yagisawa H, Hirata H. Redox regulation of lipopolysaccharide (LPS)-induced interleukin-8 (IL-8) gene expression mediated by NF kappa B and AP-1 in human astrocytoma U373 cells. Biochem Biophys Res Commun 232:568–573 (1997).
52. Beetz A, Peter RU, Oppel T, Kaffenberger W, Rupec RA, Meyer M, van Beuningen D, Kind P, Messer G. NF-kappaB and AP-1 are responsible for inducibility of the IL-6 promoter by ionizing radiation in HeLa cells. Int J Radiat Biol 76:1443–1453 (2000).
53. Tsai EY, Jain J, Pesavento PA, Rao A, Goldfeld AE. Tumor necrosis factor alpha gene regulation in activated T cells involves ATF-2/Jun and NFATp. Mol Cell Biol 16:459–467 (1996).
54. Collins T, Read MA, Neish AS, Whitley MZ, Thanos D, Maniatis T. Transcriptional regulation of endothelial cell adhesion molecules: NF-kappa B and cytokine-inducible enhancers. FASEB J 9:899–909 (1995).
55. Srebrow A, Muro AF, Werbajh S, Sharp PA, Kornblihtt AR. The CRE-binding factor ATF-2 facilitates the occupation of the CCAAT box in the fibronectin gene promoter. FEBS Lett 327:25–28 (1993).
56. Brindle PK, Montminy MR. The CREB family of transcription activators. Curr Opin Genet Dev 2:199–204 (1992).
57. Delmas V, Molina CA, Lalli E, de Groot R, Foulkes NS, Masquilier D, Sassone-Corsi P. Complexity and versatility of the transcriptional response to cAMP. Rev Physiol Biochem Pharmacol 124:1–28 (1994).
58. Morooka H, Bonventre JV, Pombo CM, Kyriakis JM, Force T. Ischemia and reperfusion enhance ATF-2 and c-Jun binding to cAMP response elements and to an AP-1 binding site from the c-*jun* promoter. J Biol Chem 270:30084–30092 (1995).